

# High-Throughput Computational and Experimental Techniques in Structural Genomics

Mark R. Chance,<sup>1,2,3,4,6</sup> Andras Fiser,<sup>1,3</sup> Andrej Sali,<sup>1,5</sup> Ursula Pieper,<sup>1,5</sup>  
Narayanan Eswar,<sup>1,5</sup> Guiping Xu,<sup>1,3</sup> J. Eduardo Fajardo,<sup>1,3</sup>  
Thirumuruhan Radhakannan,<sup>2,4</sup> and Nebojsa Marinkovic<sup>2,4</sup>

<sup>1</sup>New York Structural Genomics Research Consortium, <sup>2</sup>Department of Physiology and Biophysics, <sup>3</sup>Department of Biochemistry, and <sup>4</sup>Center for Synchrotron Biosciences, Albert Einstein College of Medicine, Bronx, New York 10461, USA; <sup>5</sup>Departments of Biopharmaceutical Sciences and Pharmaceutical Chemistry and California Institute for Quantitative Biomedical Research, University of California San Francisco, San Francisco, California 94143, USA

Structural genomics has as its goal the provision of structural information for all possible ORF sequences through a combination of experimental and computational approaches. The access to genome sequences and cloning resources from an ever-widening array of organisms is driving high-throughput structural studies by the New York Structural Genomics Research Consortium. In this report, we outline the progress of the Consortium in establishing its pipeline for structural genomics, and some of the experimental and bioinformatics efforts leading to structural annotation of proteins. The Consortium has established a pipeline for structural biology studies, automated modeling of ORF sequences using solved (template) structures, and a novel high-throughput approach (metalloomics) to examining the metal binding to purified protein targets. The Consortium has so far produced 493 purified proteins from >1077 expression vectors. A total of 95 have resulted in crystal structures, and 81 are deposited in the Protein Data Bank (PDB). Comparative modeling of these structures has generated >40,000 structural models. We also initiated a high-throughput metal analysis of the purified proteins; this has determined that 10%–15% of the targets contain a stoichiometric structural or catalytic transition metal atom. The progress of the structural genomics centers in the U.S. and around the world suggests that the goal of providing useful structural information on most all ORF domains will be realized. This projected resource will provide structural biology information important to understanding the function of most proteins of the cell.

The complete genomes of a number of organisms have been sequenced and many more are underway. This progress in gene sequencing has shifted the landscape of biology, such that goals related to understanding the structure and function of each gene product, as well as their interactions within the cellular environment that lead to the behavior of complex systems are within reach, or at least to be contemplated. The sequencing of model organisms from bacterial species to human has allowed the identification of genes both essential to function, as well as genes that give rise to the diversity of life forms. Although the exact numbers and natures of the genes is still open to question, recent estimates place the numbers at <20,000 for *Caenorhabditis elegans* and *Caenorhabditis briggsae* and ~30,000 for humans (Waterston et al. 2002; Stein et al. 2003). Our ability to recognize genes, their exons and introns, and their potential splice variants, has matured dramatically. This progress has driven highly successful attempts to develop resources to make available ORFs for rapid and highly parallel structural and functional studies of genes (Reboul et al. 2003). The success of these efforts are outlined in this issue, and the leveraging of these ORF sequences to examine protein activity, localization, protein structure, and protein-protein interactions are examples of the value of these resources. Structural biology faces the task of characterizing the shapes and dynamics of the encoded proteins to facilitate the understanding of their functions and mechanisms of action. These ORF resources will ultimately be critical to the success of the nascent

structural genomics initiatives that are underway, both in the U.S. and worldwide (Burley et al. 1999; Chance et al. 2002; Lesley et al. 2002; Burley and Bonanno 2003; Gerstein et al. 2003; Goulding et al. 2003; Shi et al. 2003; Terwilliger et al. 2003; Zhang and Kim 2003).

The Protein Structure Initiative (PSI) funded by the National Institute of General Medical Sciences ([www.nigms.nih.gov/psi](http://www.nigms.nih.gov/psi)) includes the structural genomics efforts of nine centers in the United States. In the so-called phase 1 of the PSI (Editorial 2004) these multi-institutional collaborations, along with six additional structural genomics centers in Europe and Japan, are building and developing infrastructure to provide integrated pipelines such that in phase 2, beginning in 2005, the goal of providing useful three-dimensional models for most of the known protein sequences can be vigorously pursued. The goal is to be accomplished by selecting and experimentally determining 10,000–15,000 protein structures using X-ray crystallography or NMR spectroscopy. The ORF target selection will be carried out such that at least one representative structure will be solved for most protein families. This solved structure will be used as a structural template to generate all atom-comparative protein models for the other members of the ORF family (Baker and Sali 2001; Vitkup et al. 2001). Each center in the PSI is responsible for developing and testing an integrated structural genomics effort that includes ORF target selection, cloning, expression testing, protein purification, structure solution, and modeling. This effort has required close coordination within the centers in terms of task assignment and monitoring progress, as well as coordination among the centers to maximize the effectiveness of target selection. The latter has been facilitated by the development of a

**Corresponding author.**

**E-MAIL** [mrc@aecom.yu.edu](mailto:mrc@aecom.yu.edu); **FAX** (718) 430-8587.

Article and publication are at <http://www.genome.org/cgi/doi/10.1101/gr.2537904>.

database, Target DB (<http://targetdb.pdb.org>), which lists the selected targets and progress for all of the centers in a queryable form (Westbrook 2003). This database allows the centers and the NIH to monitor overlap in target selection and has allowed many scientists outside of the centers to access information on proteins of interest to their research programs.

As a rule, the ORF targets selected for the structural genomics efforts are <30% identical (across a reasonable length) to proteins already deposited in the PDB (Sali 1998; Burley et al. 1999; Baker and Sali 2001; Vitkup et al. 2001; Chance et al. 2002; Sali et al. 2003; Shi et al. 2003). This general rule originates from the observation that reliable models can usually be constructed from structural templates that have >30% identity to the sequence of interest. In this initial phase of structural genomics projects, a major emphasis has been placed on throughput, and most structures have arisen from prokaryotic and lower eukaryotic genomes for two major reasons. First, for bacterial and yeast genes, the cloning strategies can be easily executed by each of the centers. Second, the gene products from lower organisms are to a greater degree comprised of small, soluble domains that are easily expressed and purified from bacterial systems. As progress continues, and reliable models for a large fraction of sequence space accessed through structural solution for lower organisms appear, pressure to apply high-throughput methods to gene products from higher organisms will increase. Clearly, comprehensive cloning strategies for higher organisms are more complicated. Thus, the availability of cloning vectors for orthologs from a variety of organisms will remove an important limiting factor in the progress of the overall PSI. Thus, ORF projects such as those outlined in this issue will become increasingly important to structural genomics.

The major benefit from structural genomics efforts is the provision of structural models for biologists to understand gene function. In addition, the wealth of structural information will be used to address issues of protein folding, protein structure prediction, and protein evolution. In terms of biomedical impact, the structural data will facilitate design of therapeutic agents by comparing functionally similar protein structures of pathogens and hosts, or proteins in diseased and normal tissues. The structural genomics efforts have facilitated technical developments in structure determination and the establishment of high-throughput facilities for the use of a wide community of scientists. Also, the structural genomics projects are providing reagents and materials for spin-off projects that examine function *in vivo* and *in vitro*. Lastly, retrospective analyses using the unprecedented volume of high-throughput experiments are helping to establish methods to predict experimental outcomes for protein production and crystallization. In this report, we outline the progress of the New York Structural Genomics Consortium (NYSGXRC, [www.nysgxrc.org](http://www.nysgxrc.org)) in implementing and developing its structural genomics pipeline. We emphasize the coordination of bioinformatics efforts with the experimental methods of the consortium, including the development of an integrated consortium database to manage the workflow, the overall progress from cloning to modeling, the impact of the modeling of NYSGXRC structures, and novel experimental and bioinformatics approaches to examining the structure of metalloproteins, termed metallomics (Hasnain 2004; Szpunar 2004).

## RESULTS AND DISCUSSION

### Design and Use of an Online Experimental Database

One of the key features in the successful internal functioning of the NYSGXRC (and any large multi-task project) has been the development of a database for effective communication among

the participants. The Integrated Consortium Experimental Database (IceDB) has been set up to facilitate data management among the various research groups in the NYSGXRC. IceDB fulfills several roles; it serves as a Laboratory Information Management System (LIMS) for exchanging, querying, displaying, and archiving experimental and bioinformatics data; it is used as an automated and versatile bioinformatics tool for bioinformatics screening and analysis; and finally, it is an interface and data exchange platform for users, other centers, and external resources. The system technically is a MySQL relational database that is organically interconnected with a series of locally implemented bioinformatics programs and external databases. The relational database can be accessed through a Web interface at [www.nysgxrc.org](http://www.nysgxrc.org). It is coded in HTML and Perl CGI languages.

IceDB is composed of two main parts, Target List and Progress Report. Target List contains the potential targets and their annotations in order to aid target selection. Several bioinformatics programs have been implemented for screening, such as calculating peptide statistics, predicting secondary structure, membrane immersed, and disordered regions from the sequences. Progress Report collects and displays the experimental data, and tracks the progress for all the selected targets. The collected experimental data include fields such as cloning, expression, biophysical characterization, crystallization, X-Ray data collection, X-Ray refinement, X-Ray structure, and PDB deposition. Users can insert comments and actual data (graphs, images) as appropriate for each class of field. IceDB automatically generates weekly progress statistics and XML-formatted progress reports for TargetDB, the centralized database of the PSI. IceDB also compares regularly and systematically all the active targets in the internal pipeline with the ones in TargetDB, and identifies potential overlapping cases, the extent of their sequential overlap and similarity, and the stages of experimental progress toward these structures.

IceDB interfaces with three major external resources and several public databases. This cross-linking is essential to consortium communication, as specific tasks in the structural genomics pipeline are distributed among various independent laboratories. For example, ORF target-selection bioinformatics tasks are primarily carried out at UCSF in the Sali laboratory. A list of curated ORF targets is then transmitted to the large-scale cloning and protein production facilities at Structural Genomics (SGX) in San Diego, where the overall Consortium's effort is directed by Stephen Burley. IceDB regularly exchanges data with the LIMS of SGX. Thus, data generated at SGX on cloning, expression, solubility, and purification of protein targets is automatically uploaded. Purified ORF targets are shipped from SGX to the four crystallographic laboratories in New York for automated crystallization, and these labs use IceDB to track progress in generating crystals and assessing diffraction quality upon preliminary synchrotron data collection. In this way, the crystallography laboratories receive necessary information on the targets from SGX, and SGX can determine which ORF targets are showing progress through the pipeline.

To keep track of structure solution activity at the National Synchrotron Light Source, IceDB automatically communicates with the Automated Structure Determination Platform (ASDP). ASDP is used for high-throughput X-ray structure determination subsequent to data collection (Chance et al. 2002). As the crystallography laboratories complete refinements and deposit their structures in the PDB, they periodically update IceDB. Finally, IceDB is connected to the external resource MODBASE, a comprehensive database of comparative protein-structure models, where the computational model building takes place using the newly solved ORF target structures (Eswar et al. 2003; Pieper et al. 2004). Beside these major platform hubs, which are directly re-

sponsible for facilitating major steps in the experimental pipeline, sequence and structure-based functional annotations are implemented for analysis. Target proteins in IceDB are also linked to their entries in SWISS-PROT, GenBank, and Pfam databases.

### Output of NYSGXRC Pipeline to Date and Worldwide Progress in Structural Genomics

The current progress report of the NYSGXRC as of May 2004 is shown in Table 1 and can be seen on the first page of the Web site. IceDB currently contains information about 40,000 potential ORF targets, of which 1869 are active along various stages in the experimental pipeline. To date, 1077 ORF targets have been cloned, and expression is observed for 787 of the targets. From these expressing vectors, 493 proteins have been purified and initial crystallization screens have been attempted for each. A total of 235 of the purified proteins (or 48%) have produced some form of crystal with 141, or 29%, producing diffraction quality crystals. Of these diffraction quality crystals, 95 (or 19%) have been solved to date, and 81 have been deposited to the PDB as of May 11, 2004.

Among the first 65 NYSGXRC target structures solved, 53 have been classified by SCOP (Murzin et al. 1995; Andreeva et al. 2004). Of the total, 13 have segregated  $\alpha$  and  $\beta$  structure, 23 have alternating  $\alpha$  and  $\beta$ , 11 are all- $\beta$ , and six are all- $\alpha$  protein classes. At the fold level, the 53 structures are distributed among 36 fold types. The solved targets were also compared with already known structures using the DALI program (Holm and Sander 1995, 1996). A new fold was assumed if DALI reported a Z-score of  $<10$  for the best hit. Using this cutoff value, 15 of the 65 targets (or 23%) were new folds at the time of submission. This fraction of new folds is several times higher than is generally seen for recently submitted PDB structures. (In the last 5 yr, 3%–5% of all submitted structures were classified as new folds according to SCOP). Of the 25 functionally uncharacterized proteins among the targets, seven are not classified at all in SCOP, whereas the remaining 18 are distributed among four different SCOP classes and 16 fold types.

On the basis of our current protein production rates, we now have sufficient statistics to reliably estimate the NYSGXRC output in the immediate future. The above statistics argue that ~20% of the soluble proteins delivered to the four crystallography laboratories in New York are producing crystal structures. There is, of course, a delay between the delivery of proteins and structure solution, thus, the current figure of 19% is likely to be adjusted upward as progress on targets in the pipeline continues to accrue. Nevertheless, in the fourth year of the Consortium's operation, SGX has delivered 192 soluble targets as of March 2004 and will

deliver 350 additional targets by September 2004, the end of the fourth year. On the basis of our progress to date, we expect that >100 new structures will be solved from these ORF targets. SGX plans to supply the crystallography laboratories with ~50 soluble targets per month throughout the fifth year of the project; 120 structures are ultimately expected to be produced from these targets. On the basis of this productivity level, the NYSGXRC is poised to achieve its initial goal of producing at least 100 structures in its fifth year of operation.

The production statistics for the 15 structural genomics centers located around the world as of May 2004 include 28,293 proteins cloned with expression observed in 16,468 of the vector targets (or 58%). A total of 6177 targets have been seen to produce soluble protein, from which 5924 proteins have been purified. Thus, the overall experience is that purified protein has been obtained from 36% of the vectors for which expression has been observed. A total of 2162 of the purified proteins formed crystalline material, and 1034 (17% of the purified target set) resulted in diffraction quality crystals, whereas 715 structures have been deposited to the PDB. These outcomes are expected to improve, as some of the proteins are still at some intermediate stage in the various pipelines. Compared with the goal of producing 10,000–15,000 new structures to provide completeness in structural genomics (Vitkup et al. 2001), this is merely a down payment, but represents promising initial progress. If we can rely on the above metrics that suggest 20% of purified proteins will produce diffraction quality crystals, then 50,000–75,000 proteins will need to be purified in order to achieve an overall goal exceeding 10,000 structures. However, the calculation that one-third of the expressing vectors may provide easily purifiable protein may not hold for multidomain proteins from higher organisms (Burley et al. 1999; Chance et al. 2002), at least not without methodological improvements in expression systems. However, it sets a likely lower limit of 200,000 expression vectors that will need to be constructed to complete the overall project.

### Modeling NYSGXRC Sequences: How Structural Models Are Informing New Biology

Recent developments in the techniques of structure determination at atomic resolution, X-ray diffraction, and nuclear magnetic resonance spectroscopy, have enhanced the quality and speed of structural studies (Zhang and Kim 2003). Nevertheless, current statistics still show that the known protein sequences (~1,500,000; Boeckmann et al. 2003) vastly outnumber the available protein structures (~25,000; Westbrook et al. 2002). Fortunately, domains in protein sequences are gradually evolving entities that can be clustered into a relatively small number of families with similar sequences and structures (i.e., folds; Vitkup et al. 2001). These evolutionary relationships enable the use of computational methods, such as threading and comparative protein structure modeling (Fiser et al. 2001), to predict the structures of protein sequences on the basis of their similarity to known protein structures. The NYSGXRC is combining experimental structure determination methods with computational modeling techniques. This effort, combined with that of other structural genomics centers worldwide, aims to determine a sufficient number of appropriately selected structures, so that most ORF sequences can be placed within modeling distance of at least one known structure (Sali 1998; Sanchez and Sali 1998; Baker and Sali 2001; Vitkup et al. 2001).

A suite of bioinformatics programs and databases is at the foundation of the NYSGXRC's computational efforts. MODBASE (<http://salilab.org/modbase>) is a comprehensive database of annotated comparative protein structure models (Pieper et al.

**Table 1.** Progress of NYSGXRC as of May 2004, Updates Available at [www.nysgxrc.org](http://www.nysgxrc.org)

Targets selected	1869
Cloned	1077
Expression successful	787
Soluble	581
Purified	493
Crystallized	235
Diffraction-quality Crystals	141
Native diffraction-data	98
Phasing diffraction-data	98
Crystal Structure Complete	95
Deposited in PDB	81

2004). MODBASE models are calculated by MODPIPE (Eswar et al. 2003), a fully automated comparative protein structure modeling pipeline. MODPIPE relies on various modules of the comparative modeling software MODELLER (Sali 1995) for its functionality, and is streamlined for large-scale operations on a cluster of PCs. The modeling process comprises the following steps: fold assignment, sequence-structure alignment, model building, and model assessment. MODBASE is updated regularly to reflect the growth in sequence and structure databases, as well as improvements in the software for calculating the models.

MODBASE is organized into several model data sets. The largest contains models for domains in 659,495 sequences of 1,182,126 unique protein sequences in the complete SWISS-PROT/TrEMBL (Boeckmann et al. 2003) database (August 25, 2003). These models correspond to all known protein sequences in SWISS-PROT/TrEMBL that can be matched to at least one known protein structure. The second largest group of model data sets includes MODPIPE models for the SWISS-PROT/TrEMBL sequences that were modeled on the basis of the NYSGXRC structures. We run MODPIPE using all NYSGXRC structures as templates to contribute to their annotation. When a new consortium structure is deposited in the PDB, a MODPIPE run using this new structure as a template is automatically triggered, and models for all sequences in SWISS-PROT/TrEMBL that are related to this structure are calculated. These calculations are repeated periodically for all template structures. All protein sequences in SWISS-PROT/TrEMBL that are related to the NYSGXRC structures can be viewed in MODBASE.

Relying on the first 63 unique NYSGXRC solved structures, MODPIPE produced models for domains in 33,340 sequences in SWISS-PROT/TrEMBL (Table 2). The modeled sequences come from 2676 different organisms, with a kingdom distribution of 41% Prokaryota, 2% Archaea, and 57% Eukaryota. This organism classification has been derived from the NCBI taxonomy database, where all protein sequences are matched with a taxonomy id (Wheeler et al. 2000; Benson et al. 2002). The average ORF target-template sequence identity was 18.6%. Only 10% of the sequences are modeled on the basis of >30% sequence identity over more than 75 residues; 81% of the sequences have models that are predicted to have the correct fold on the basis of the model score (John and Sali 2003) or the PSI-BLAST E-value (Schaffer et al. 2001). Using these data sets, all amino acid sequences in SWISS-PROT/TrEMBL that are related to the NYSGXRC structures can be viewed in MODBASE, which easily facilitates the detection of remote relationships and the annotation of function to proteins previously annotated as hypothetical proteins.

Considering that the target sequences for NYSGXRC were selected to have <30% sequence identity to a known experimental structure, most of the modeled ORF sequences have been characterized structurally for the first time. Thus, these data sets indicate the increased coverage of the sequence-structure space by the NYSGXRC structures. In fact, the experience so far for the U.S. centers is that 70% of their PDB deposits in 2002–2003 are for proteins containing unique sequences, (i.e., sequences with <30% sequence identity to the closest known structure) compared with only 10% of the deposits overall during the same time period (Editorial 2004). The large number of new models that can be calculated on the basis of the newly determined structures illustrates and justifies the premise of structural genomics.

The most interesting cases for functional analysis would be proteins for which sequence-based methods failed to establish a meaningful connection to a protein of known function or structure. On the basis of our current experience, every third target solved in the NYSGXRC pipeline remains functionally uncharacterized. These proteins are ripe for experimental investigation using biochemical or genetic approaches. Although funds are

available from the NIH for the study of functionally characterized structures solved by the PSI centers, no mechanism exists to systematically study the uncharacterized proteins (Editorial 2004).

Another way to glean functional insight for unannotated protein structures is through the comparative modeling pipeline. Structure-based search and confirmation of protein relationship is usually more reliable and sensitive than sequence-only based approaches. Such structural (and potentially functional) assignments are called “nontrivial hits” (summarized in Table 2 in the M column), and are usually based on very low (<20%) sequence identity between aligned regions of the target and template sequences. An example is the model of a protein sequence annotated in the TrEMBL database (Boeckmann et al. 2003) as “Hypothetical protein SCP1.152” (Bentley et al. 2002; TrEMBL accession no. Q9ACZ9, organism: *Streptomyces coelicolor*) that was modeled using the PDB structure 1rvk (NYSGXRC target T1522). The sequence identity between 1rvk and Q9ACZ9 is 19%, the PSI-BLAST E-value is 0.1, and the model score 0.71. The model covers 91 of 104 amino acid residues. 1rvk has been annotated as isomerase/lactonizing enzyme. The modeling results suggest that Q9ACZ9 has a similar function. This specific example illustrates that structure modeling can identify functional similarities between ORF sequences that lack any detectable sequence similarity.

### High-Throughput Annotation of Metal-Binding Targets

An interesting conclusion from the production statistics above is that if ~20% of the soluble ORF targets are ultimately amenable to structural analysis, ~80% of the proteins are not, and represent ORF targets that are likely to be abandoned. However, these proteins present a potentially valuable resource for spectroscopic and biochemical analysis to better understand structure and function. In general, the consortium has pursued a limited number of approaches to provide characterization of target proteins. This has included light scattering and limited proteolysis mass spectrometry (Burley et al. 1999; Shi et al. 2003). The former is to determine whether the protein preparations are mono-disperse, as such a preparation is much more amenable to crystallization. The latter is to determine whether the purified ORF target represents a compact globular domain, which also crystallizes much more efficiently. This information is used to inform protein-purification strategies in the case of poly-disperse samples, and is used to direct recloning efforts in the case of exposed protease sensitive sites. However, these analyses do not give major insights into structure and function. To provide additional annotation to ORF targets, we have implemented an automated system to analyze all purified ORF targets for transition metal content. This effort has multiple purposes. First, identification of metal binding can be used to make the protein purification and protein-crystallization strategies more efficient by supplementing the buffers with the metal in question. Second, identification of metal binding can be used to aid in annotation of protein function, especially for so-called “hypothetical” proteins. Third, for proteins that crystallize, the intrinsic transition metal can, in favorable cases, be used for anomalous scattering phasing of the structure (Hendrickson 1991; Rajashankar et al. 2001).

Up to one-third of proteins contain metal atoms (Hasnain 2004; Szpunar 2004) with iron and zinc being the most common among the transition metals (Lujan et al. 1995). Protein samples illuminated with high-energy synchrotron X-rays eject a 1s electron from the first electron shell surrounding a metal nucleus (Fig. 1). Passage of another electron from a higher shell to fill the hole in the first shell yields an emitted X-ray photon (fluores-

**Table 2. MODBASE Model Data Sets Using the PDB Structures of the First 63 Released and Unique NYSGXRC Targets as Templates**

PDB code	Target Id	Database Accession	Annotation	No. of Sequences			
				Total	FM	M	F
1b54	P007	P38197	Hypothetical UPF0001 protein YBL036C	151	132	17	2
1ci0	P008	P38075	Pyridoxamine 5'-phosphate oxidase (EC 1.4.3.5)	99	93	0	6
1dfc	P119	11513471	Fascin (Singed-like protein) (p55)	81	27	32	22
1f89	P018	P49954	Hypothetical 32.5 kDa protein YLR351C	547	488	10	55
1fi4	P100	P32377	Diphosphomevalonate decarboxylase (EC 4.1.1.33)	154	64	88	5
1g61	P111a	Q60357	Translation initiation factor 6 (aIF-6)	49	46	2	1
1g62	P111	Q12522	Eukaryotic translation initiation factor 6 (eIF-6)	51	50	1	0
1hqz	T138	113000	ABP1_YEAST actin binding protein	175	50	124	2
1i9a	P109a	6225535	IDI_ECOLI isopentenyl-diphosphate delta-isomerase	1140	510	11	619
1jd1	P003	P40037	HMF1 protein (High dosage growth inhibitor)	382	354	3	26
1jf9	T129	P77444	Selenocysteine lyase (EC 4.4.1.16)	1669	1616	0	54
1jfi	P048a	7513394	S70618 transcription regulator NC2 alpha chain	86	15	0	71
1jg8	P044a	4982322	L-allo-threonine aldolase	1611	1461	69	123
1jr7	T130	P76621	Hypothetical protein ygaT	11	10	1	0
1jss	T526	13542895	Similar to RIKEN cDNA 2310058G22 gene	254	176	2	76
1jsx	T35	121191	GIDB_ECOLI glucose inhibited division protein B	1583	1064	27	496
1jyh	T473	465566	GYRI_ECOLI DNA gyrase inhibitory protein	144	97	0	47
			Hypothetical 27.5 kDa protein in SPX19-GCR2				
1jzt	P097	P40165	intergenic region	1058	39	13	1006
1k47	T27	9937409	phosphomevalonate kinase	539	385	33	124
1k4z	T139	399184	CAP1_HUMAN adenyl cyclase associated protein	44	34	8	2
1k8f	T140	134897	CAP_YEAST adenyl cyclase associated protein	48	36	10	2
1kag	T535	P24167	Shikimate kinase I (EC 2.7.1.71) (SKI)	1005	250	51	706
1kcx	T45	2342488	dihydropyrimidinase related protein 1	701	378	20	312
1ku9	T136	3025177	YF63_METJA HYPOTHETICAL PROTEIN MJ1563	572	131	253	214
1l9g	T299	Q9WY1	Hypothetical protein TM0511	170	152	3	15
1la2	T23	P11986	Inositol-3-phosphate synthase (EC 5.5.1.4) (IPS)	102	86	0	16
1lnz	T131	P20964	Spo0B-associated GTP-binding protein	1620	960	40	678
1lx7	T24	P12758	Uridine phosphorylase (EC 2.4.2.3) (UDRPase)	506	384	1	121
1m0t	P102	Q08220	Glutathione synthetase (EC 6.3.2.3) (GSH-S)	38	37	1	1
1m0w	P102a	Q08220	Glutathione synthetase (EC 6.3.2.3) (GSH-S)	39	38	0	1
1n10	T467	28373838	Phl P 1, A Major Timothy Grass Pollen Allergen	358	336	9	13
1ne8	T503	P96622	YDCE protein	111	84	21	6
1ni3	T9	O13998	Similar to putative GTP-binding protein	1058	103	1	955
1ni5	T132	P52097	Putative cell cycle protein mesj	920	204	40	689
			Hypothetical 32.1 kDa protein in ADH3-RCA1				
1njr	P089	Q04299	intergenic region	4	1	3	0
			Hypothetical 28.8 kDa protein in PSD1-SKO1				
1nkq	P096	P53889	intergenic region	379	207	0	172
1nlx	T746	P43215	Pollen allergen Phl p 6 precursor (Phl p VI)	12	12	0	1
1nr0	T745	Q11176	Actin interacting protein 1 (AIP1)	752	633	33	142
1nvt	T576	Q58484	Shikimate 5-dehydrogenase (EC 1.1.1.25)	543	189	348	7
1omi	T143	P22262	Listeriolysin regulatory protein	1094	301	7	798
1p1l	T835	O28301	Periplasmic divalent cation tolerance protein (CUTA)	68	63	0	5
1p1m	T834	Q9X034	Hypothetical protein TM0936	780	354	24	404
1pb6	T803	P75899	Hypothetical transcriptional regulator ycdC	1364	1152	74	155
1pqw	T109	7448840	A70984 probable polyketide synthase	1496	1426	39	35
1pqy	T783	P77407	Hypothetical protein yfdW	607	579	11	23
1psq	T817	P72500	Probable thiol peroxidase	950	664	23	263
1psu	T820	O28020	Hypothetical protein AF2264	662	244	26	393
1psw	T832	Q51063	ADP-heptose:LPS heptosyltransferase II	642	258	229	194
1pug	T5	P17577	Hypothetical UPF0133 protein ybaB	118	112	6	0
1pui	T16	P24253	Probable GTP-binding protein engB	1380	925	52	438
1puj	T18	O31743	YLQF protein	1128	96	20	1012
			Hypothetical 33.9 kDa esterase in SMC3-MRPL8				
1pv1	P068	P40363	intergenic regionDE (EC 3.1.1.-)	143	36	14	93
1q2y	T804	O31628	YJCF protein	1676	1123	121	479
1q6w	T805	Q28346	Monoamine oxidase regulatory protein, putative	566	279	14	285
1q98	T1429	Q57549	Probable thiol peroxidase (EC 1.11.1.-)	1218	763	19	436
1q9j	T760	P96208	Hypothetical protein papA5	694	32	3	671
1r3d	T920	Q9KQM4	Hypothetical protein VC1974	1602	563	20	1030
1rc6	T1521	16128499	Hypothetical protein ylbA	474	50	46	382
1ri6	T1479	16128735	Hypothetical protein ybHE	1458	350	1126	77
1rvk	T1522	17937161	isomerase/lactonizing enzyme	1115	864	139	124
1s7j	T1581	29374770	Phenazine biosynthesis protein PhzF family	361	236	124	1
1ub4C	T1468	126777	PemI-like protein 1 (MazE protein)	40	9	8	23
1ub4A	T1469	464357	PemK-like protein 1 (MazF protein)	112	99	8	5

The PDB code, Database Accession, and Annotation columns define the template structure. (No. Sequences) The number of sequences in SWISS-PROT/TrEMBL that could be modeled reliably using the NYSGXRC structure as a template. (Total) The total number or sequences, (F) the number of sequences that have a reliable PSI-BLAST E-value of  $\leq 10^{-4}$  but a low model reliability score ( $<0.7$ ), (M) the number of sequences with a model score  $\geq 0.7$  (reliable model), but with insignificant PSI-BLAST E-value ( $>10^{-4}$ ), (FM) the number of sequences that have both a reliable model score and a significant PSI-BLAST E-value. The most reliable models have both a reliable PSI-BLAST E-value and a reliable model score (FM). For the models classified as F, the fold assignment is considered reliable, even though the model score is bad. Models classified as M have only a remote relationship to the template, but the good model score suggests that the modeled sequences indeed have the same fold as the template structure. The full table can be viewed at [http://salilab.org/modbase/models\\_nysgxrc.html](http://salilab.org/modbase/models_nysgxrc.html).

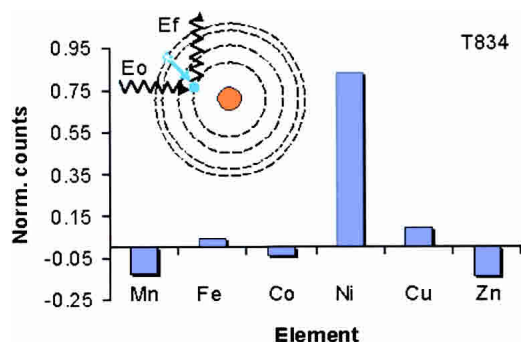


**Figure 1** The corrected fluorescence counts for each metal atom are shown in histogram format (i.e., sample well counts minus counts from a blank well). The corrected counts for nickel are very far above background. The inset shows electron orbitals in schematic form with incident X-ray, the transition from higher to lower energy orbitals, and emission of X-ray fluorescence illustrated. The incident X-ray ( $E_0$ ) knocks out a 1s electron, the unstable core hole is filled by the subsequent transition (seen in color), and a fluorescent X-ray of energy characteristic for the metal atom is emitted ( $E_f$ ).

cence emission) with energy characteristic for the individual elements (Chance et al. 1992; Summers et al. 1992; Lujan et al. 1995). We have developed an automated system to scan and detect transition metal content of protein target samples in 16-well plates with a multiplate rail and precise and automated alignment of the samples in a synchrotron X-ray beam. Detection of fluorescent emitted photons is accomplished with a multi-element, fast count rate, high-resolution Germanium detector (Summers et al. 1992; Lujan et al. 1995). Although all elements in the sample will emit fluorescence given sufficiently high energy X-rays incident on the sample, practical considerations of sample thickness and air absorption limit the analysis, in this case, to the following transition elements: Mn, Fe, Co, Cu, Ni, and Zn; however, data collection times are only a few minutes per sample for nanogram detection efficiencies.

We analyzed 143 proteins from prokaryotic sources recently delivered by SGX to the crystallography laboratories for crystallization testing. For each protein, 200  $\mu$ g of sample were loaded onto the sample plates and dried under controlled conditions. The results in terms of corrected counts for T834, which was annotated as a hypothetical protein (Table 3), are shown in Figure 1. The sample showed significant nickel fluorescence counts, but minimal amounts of the other metals were detected. Of the 143 samples examined, >20 indicated some transition metal content (data not shown). To limit the analysis to likely cases of structural or functional metal atoms, the metal-to-protein stoichiometry was determined by comparison of the corrected counts with an appropriately chosen set of standards for each metal at the same experimental conditions; thus, the number of moles of each metal was accurately measured. The results for the 16 proteins that showed a metal/protein ratio of 0.7 or greater are shown in Table 3; the error in this analysis is  $\pm 0.2$ , such that we report data only for metal binding that is likely to be stoichiometric, and therefore relevant. Of these, two proteins contain two or more metal atoms per protein molecule, and 14 proteins contain one or more metal per molecule (metal/protein ratios 0.7–1.6), including T834. Zinc was observed in eight cases, copper and nickel in three each, and iron and manganese once.

In the following section, we examine the known annotations for these 16 proteins. Our analysis is likely to emphasize false negatives, as some metalloproteins may lose a metal atom in the purification step. We have already excluded one false positive, where a stoichiometry of 0.5 Zn/protein was observed for

T1429 (data not shown, AC:Q57549). This target was solved by the NYSGXRC (1q98). An anomalous difference Fourier analysis showed no evidence of a metal atom signature. However, this protein does have exposed Cys residues that may be able to coordinate adventitious Zn during the purification. This is one factor leading to the choice of a cutoff of 0.7 metal/protein for the annotation of metalloprotein identity.

### Functional Annotation of Metal-Binding Proteins

The 16 NYSGXRC target protein sequences that are strongly indicated to be metalloproteins were retrieved from IceDB, and bioinformatics analysis was carried out to analyze the consistency of the metal binding with known annotations. Table 3 shows the target IDs, the SWISS-PROT or GenBank identifier, the annotation as provided by IceDB, additional annotations from relevant databases, and the organism from which the target is derived (Boeckmann et al. 2003). A BLAST search was carried out against SWISS-PROT to identify closely related homologs. For T834 (0.8 Ni/protein), the BLAST search revealed a related hypothetical protein and similarity to members of the Atz/Trz family. Clusters of Orthologous Groups (COG) was examined; these results are shown in Table 3. For T834, this search indicated a close relationship with cytosine deaminases and related metal-dependent hydrolyases. The crystal structure of this protein was solved within the NYSGXRC (1p1m) and a single Ni ion was confirmed as part of the structure (PDB data in Table 3). Thus, in this case, the metal analysis was supported by bioinformatics comparisons and direct structure determination.

For T763, a zinc/protein stoichiometry of 1.3 was measured; the protein was annotated as a putative amidohydrolyase. The BLAST search indicated a close relationship with a zinc-containing carboxypeptidase and an overall similarity with the M40 peptidase family. The COG analysis indicated that the target belongs to a metal-dependent amidase family. A search against PDB found no significant homologies. The annotation of this protein as a metalloprotein is very strongly confirmed by the bioinformatics analysis, although the crystal structure of this protein remains unsolved.

T830 is annotated as a hypothetical protein with similarity to an ADP-ribose pyrophosphatase, which is indicated to have a magnesium cofactor. The COG database also indicates that this target belongs to the same enzyme family. No similarity to any structure in the PDB was found. The annotation of T830 as a manganese-containing enzyme is reasonable, as active sites that bind magnesium generally can be exchanged for manganese. Thus, the metal analysis provides evidence that this target is a metal-dependent hydrolyase.

For T1407, T797, T1403, and T1404, the identification as metalloproteins is well supported by bioinformatics, which, in each case, provides a functional annotation (in terms of enzyme activity) consistent with metal binding by the target. T1407 (binding Ni) is annotated in the alcohol dehydrogenase family (the presence in this target of a metal-binding motif was also seen in PROSITE). A related structure in the PDB is seen to contain Fe. Zinc-containing T797 is a DNA-glycosylase closely related to PDB entry 1nku, which also contains zinc. T1404, the MazG protein and the related T1403 are indicated to have pyrophosphatase motifs consistent with zinc binding.

In several cases, the metal binding provides a new annotation for protein of unknown or not-well-understood functions. T790, indicated to contain copper, was annotated a hypothetical protein and COG indicated an uncharacterized enzyme. A related structure in the PDB is seen to contain Zn. T1405 also is listed as a hypothetical protein predicted to be related to glutamine amidotransferases; the metalloprotein annotation may assist in bet-

**Table 3.** Metal Atoms Found in NYSGXRC Target Proteins and Annotations of Targets and Closely Related Genes

Target ID	Metal	NMA	Target Annotation	Clusters of Orthologous groups	BLAST-PDB	Related Structure
T763	Zn	1.3	AC: Q9PHR1 Putative amidohydrolase OS: <i>Campylobacter jejuni</i> SIMILARITY-Peptidase Family M40.	Ev = 2e-95 Metal-dependent amidase/aminoacylase/ carboxypeptidase	No closely related structure	—
T773	Zn	0.9	AC: O34974 YTNJ OS: <i>Bacillus subtilis</i> SIMILARITY-Ntaa/Snaa/Soxa(Dsza) Family of Monooxygenases.	Ev = e-144 Coenzyme F420-dependent N5,N10-methylene tetrahydromethanopterin reductase	Ev = 7e-10 Alkanesulfonate Monooxygenase.	PDB ID: 1NQK Identity = 28% Metal ions = no
T788	Zn	4.6	AC: Q9WYG6 Orotate phosphoribosyltransferase OS: <i>Thermotoga maritima</i> SIMILARITY-Purine/pyrimidine phosphoribosyltransferase family.	Ev = e-103 2-keto-4-pentenoate hydratase/2- oxohepta-3-ene-1,7-dioic acid hydratase	Ev = 3e-06 Purine Operon Repressor of <i>Bacillus Subtilis</i> .	PDB ID: 1O57 Identity = 24% Metal ions = no
T790	Cu	0.9	AC: O06156 Hypothetical protein Rv3592 OS: <i>Mycobacterium tuberculosis</i>	Ev = 6e-57 Uncharacterized enzyme; polysaccharide synthesis	Ev = 3e-10 Tt1380 Protein	PDB ID: 1IUJ Identity = 39% Metal ions = Zn
T797	Zn	0.7	AC: P44321 DNA-3-methyladenine glycosylase OS: <i>Haemophilus influenzae</i>	Ev = e-108 3-methyladenine DNA glycosylase	Ev = 7e-67 DNA/Glycosylase I	PDB ID: 1NKK Identity = 62% Metal ions = Zn
T813	Fe	1.0	AC: Q58465 Hypothetical protein MJ1065 OS: <i>Methanococcus jannaschii</i>	Ev = 2e-74 Sialic acid synthase	There is no closely related structure	—
T818	Zn	0.7	AC: O34790 PcrB protein homolog OS: <i>Bacillus subtilis</i>	Ev = e-128 Predicted phosphate-binding enzymes, TIM-barrel fold	Ev = e-125 Hypothetical Protein.	PDB ID: 1VIZ Identity = 99% Metal ions = no
T823	Cu	1.1	AC: P24216 Flagellar hook-associated protein 2 OS: <i>Escherichia coli</i>	Ev = e-124 Flagellar capping protein	No closely related structure	—
T824	Cu	2.4	AC: Q9PNP0 Restriction modification enzyme OS: <i>Campylobacter jejuni</i>	Ev = 2e-24 Type I restriction-modification system methyltransferase subunit	No closely related structure	—
T830	Mn	1.6	AC: Q9K2H0 Hypothetical protein OS: <i>Streptococcus pneumoniae</i> SIMILARITY-Nudix Hydrolase	Ev = 6e-18 ADP-ribose pyrophosphatase	No closely related structure	—
T834	Ni	0.8	AC: Q9X034 Hypothetical protein TM0936 OS: <i>Thermotoga maritima</i> SIMILARITY - Atz/Trz Family	Ev = 1e-79 Cytosine deaminase and related metal-dependent hydrolases	Ev = 0.0 Hypothetical Protein Tm0936	PDB ID: 1P1M Identity = 100% Metal ions = Ni
T1403	Zn	1.0	AC: Q9S3S2 Beta lactamase regulatory protein homolog OS: <i>Vibrio cholerae</i>	Ev = 8e-93 Predicted pyrophosphatase	No closely related structure	—
T1404	Zn	0.8	AC: P33646 MazG protein OS: <i>Escherichia coli</i> SIMILARITY-S.CACO1 ORF in BLAB 3' Region	Ev = e-148 Predicted pyrophosphatase	No closely related structure	—
T1405	Zn	0.7	AC: O33341 Hypothetical protein Rv2859c OS: <i>Mycobacterium tuberculosis</i>	Ev = e-180 Predicted glutamine amidotransferases	No closely related structure	—
T1407	Ni	1.0	AC: P11549 Lactaldehyde reductase OS: <i>Escherichia coli</i> SIMILARITY-iron-containing alcohol dehydrogenase family.	Ev = 1e-82 Fucose permease	Ev = 7e-32 Alcohol Dehydrogenase,	PDB ID: 1O2D Identity = 30% Metal ions = 2Fe
T1421	Ni	1.5	AC: P09151 2-isopropylmalate synthase OS: <i>Escherichia coli</i> SIMILARITY-alpha-IPM synthetase	Ev = e-170 Isopropylmalate/homocitrate/citram alate synthases	There is no closely related structure	—

(NMA) Number of Metal Atoms per protein molecule; (OS) Organism/Species; (AC) Accession number; (Ev) E-value.

ter understanding its function. In other cases, the proteins have good annotations, but no indication of metal binding, and the metal content may suggest important structural or functional information. For example, T773 is annotated as a monooxygenase and the zinc ion may be related to the protein's catalytic function, or may serve as a structural metal. T788 has over 4

Zn/protein indicated; it is unclear as to how this may be related to its annotated enzyme function. However, T824, which has over 2 Cu/protein and is annotated as type-I restriction enzyme, may have metal functions directly related to the DNA cleavage mechanism of this protein. In the case of T818, the indicated zinc atom may represent a false positive, in that the structure of a

nearly identical sequence shows no metal atom or indication of a likely metal-binding site.

Overall, the metallomics analysis found many metalloproteins among the 143 proteins examined so far. On the basis of the observed annotations, the metal content was, in most cases, very reasonable, and in other cases, potentially informative with respect to protein function. Using the cutoff of measured metal/protein stoichiometry of 0.7, the rate of false positives may be in the range of from 5% to 10%. The range of false negatives cannot be estimated yet without more data. Over the next 18 mo, we expect to screen over 900 additional proteins provided by SGX, such that we can better refine these numbers.

### Conclusion: Opportunities and Limitations of the Protein Structure Initiative and the Next Challenge for Structural Biology

The NYSGXRC has assembled a robust pipeline for structural genomics research that is part of an international initiative to provide structural models for all possible ORF sequences. On the basis of current structural information in the PDB, domains in ~57% of the known protein sequences can be modeled using MODPIPE and are available in MODBASE (Sanchez and Sali 1998; Sanchez et al. 2000; Pieper et al. 2002, 2004). As the PSI expands into its second phase in 2005, the expansion of this sequence coverage will rapidly increase, providing a valuable resource for biologists worldwide.

Although this sequence coverage and the number of modeled proteins may look impressive, usually only one domain within the ORF sequence of each protein is modeled. On average, proteins have two or three domains. That is, an average yeast ORF codes for 472 amino acid residues, whereas the average size of domains in CATH (Orengo et al. 1997), a database of structural domains, is 175. The average model size in MODBASE is 192 residues, very similar to this domain size (Pieper et al. 2004). This limitation on comparative modeling is a direct consequence of the available structural templates. An additional problem is that membrane protein structures are poorly represented in PDB, whereas 15%–30% of proteins in various genomes are predicted to contain transmembrane helices (Liu and Rost 2001). It is also suggested that up to 20% of proteins contain unstructured regions, at least in the absence of their binding partners (Tompa 2002), which often makes them unsuitable for structure determination experiments. These limitations are not likely to be overcome, even on completion of the PSI. The experience of the NYSGXRC is that the average size of the proteins solved to date is ~250 residues ([www.nysgxrc.org/nysgxrc/result.html](http://www.nysgxrc.org/nysgxrc/result.html)), slightly

larger than the average domain size seen in CATH, but much smaller than the average protein size in yeast. In addition, we have few examples of transmembrane segments and unstructured regions in our solved structures; such domains are often excluded during target selection. However, ~40% of the solved targets to date are eukaryotic in origin. Thus, the expectation is that domains from a wide variety of targets may be solved in the PSI-2.

The next challenge involves understanding the domain interactions and the assembly of proteins into complexes, Figure 2 (Gavin et al. 2002; Sali et al. 2003). Whereas structural genomics aims to provide atomic resolution models for the domains that make up the proteins and complexes that are functionally relevant to cell biology, it does not explicitly address how these structures interact with each other. The interacting surfaces of the domains dock in functionally relevant ways that are amenable to experimental tools such as cryo-EM, cross-linking, footprinting, and genetic analysis (Sali et al. 2003; Guan et al. 2004; Tong et al. 2004). A next phase of structural genomics efforts will be a gradual transition to structural proteomics, when the experimental information on organization of protein complexes and domain interactions, combined with computational modeling, will be used to understand the structure and dynamics of macromolecular assemblies. Structural genomics efforts are imperative prerequisites to these future efforts.

## METHODS

### Metallomics Analysis

We irradiated samples with synchrotron X-rays produced by the NSLS X-ray ring (the ring operates at the constant energy of 2.8 GeV and current decaying with time from 280 to ~200 mA). The beamline configuration is similar to that used for focused beam X-ray absorption spectroscopy measurements (Chance et al. 1996), with the monochromator set to 10 keV, and harmonic rejection using a Ni-coated mirror. The setup consists of a multiplate rail positioned at 45° with respect to the beam that brings a sample plate in a position close to the synchrotron X-ray source, an x-z stage and two ionization chambers placed before and after the sample plate for precise alignment of a sample in the plate to the beam, and a multi-element, fast count rate, high-resolution Germanium detector placed perpendicular to the beam path, that captures the X-ray fluorescence. The detector has 13 separate elements, whose counts can be summed for signal averaging. Sufficient electronics exists, such that three metals can be analyzed using single channel analysis at a time (Lujan et al. 1995). We focus on collecting signals from the following transi-

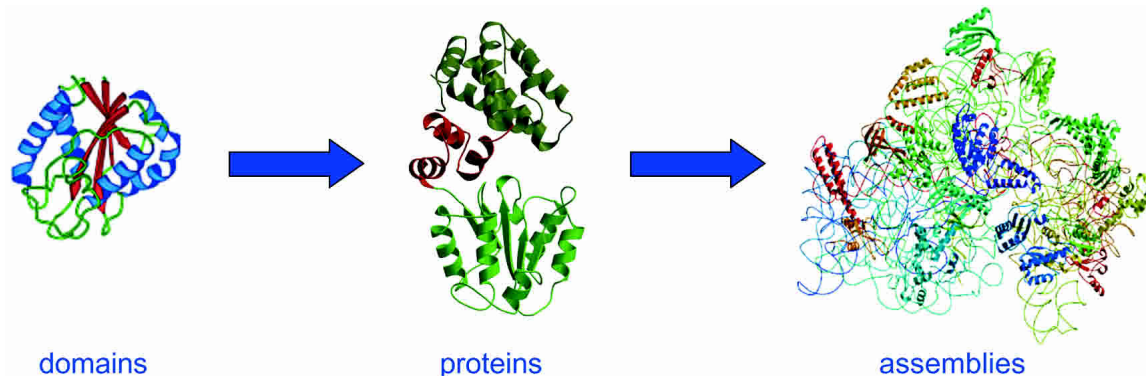


**Figure 2** Protein domains will be solved by structural genomics, the docking of domains in protein structures or the structures of assemblies will be a challenging next step for structural biology to be solved by a combination of structure modeling of domains combined with experimental data from techniques such as cryo-EM, cross-linking, footprinting, and genetic knockout analysis.



tion elements: Mn, Fe, Co, Cu, Ni, and Zn, such that two runs are required to collect all of the required data.

A total of 16 sample wells were bored in a Teflon plate, and three plates can be simultaneously loaded onto a multiplate rail. The synchrotron beam is shaped by slits to match the size of the sample well (2.5 × 6.5 mm). After loading samples in sample wells and drying them in a controlled manner, the plates are placed into the rail. The first run consists of selecting the characteristic energies for three metals using the detector software and starting an automated program that positions sample wells in front of the beam and collects the data. A total of 60, 1-sec-long counting intervals are summed. The second run screens the same set of 48 samples for another three metals. The total time to complete both runs is about 4 h, or about 4 min/sample.

The validity of the metal determinations was evaluated as follows. We have previously published methods of quantitation for metal atoms in biological samples using X-ray absorption spectroscopy (Chance et al. 1992; Lujan et al. 1995). For this experimental setup, the metal-to-protein stoichiometry was derived from standards measured before the sample data collection. Standard sets, prepared with water-soluble chlorides or nitrates of transition metals in the weight range from 0.4 to 5 µg show linear dependence of metal mass with measured fluorescence counts. Subsets of samples spiked with defined amounts of cytochrome-c were also measured to confirm the validity of the above standards on real protein samples. However, these experiments only define the measurement error and detection limit for the analysis. The decision to use a specific cutoff (0.7 metal/protein used here) for assigning a valid metalloprotein is entirely arbitrary. Setting the criteria high increases the false negatives, setting it lower (e.g., <0.5) increases the false positives. As we analyze more samples, we will get a better idea of the expected percent of each kind of error associated with a specific cutoff value.

Target sequences were retrieved from IceDB in the NYS-GXRC Web site ([www.nysgxrc.org/nysgxrc/cgi/search\\_progress\\_report.cgi](http://www.nysgxrc.org/nysgxrc/cgi/search_progress_report.cgi)), and were analyzed by PSI-BLAST searches against SWISS-PROT (Altschul et al. 1997; Boeckmann et al. 2003), Cluster of Orthologous Groups (COG; [www-archbac.u-psud.fr/genomics/COG\\_Guess.html](http://www-archbac.u-psud.fr/genomics/COG_Guess.html)), and the Protein Data Bank (Berman et al. 2000). The protein having the lowest E-value (if a candidate was found at <10<sup>-4</sup>) is selected, and the annotations are included in Table 3.

## ACKNOWLEDGMENTS

We thank Stephen Burley and Steve Almo for advice on this project and Jeff Bonnano for coordinating sample delivery from SGX. Chris Lima kindly analyzed T1429 for presence of metal atoms by anomalous difference Fourier. This research is supported primarily by a grant from the National Institute for General Medical Sciences under the PSI Program (P50-GM-62529). Additional funding is provided under R01-GM-54762 (A.S.), R33-CA-84699 (A.S.), and the National Institute for Biomedical Imaging and Bioengineering and its Biomedical Technology Centers Program under P41-EB-01979 (M.R.C.). Support from the Sander Family Supporting Foundation, Sun Academic Equipment Grant EDUD-7824-020257-US, an IBM SUR grant, and an Intel computer hardware gift are also acknowledged (A.S.).

## REFERENCES

- Altschul, S.F., Madden, T.L., Schaffer, A.A., Zhang, J., Zhang, Z., Miller, W., and Lipman, D.J. 1997. Gapped BLAST and PSI-BLAST: A new generation of protein database search programs. *Nucleic Acids Res.* **25**: 3389–3402.
- Andreeva, A., Howorth, D., Brenner, S.E., Hubbard, T.J., Chothia, C., and Murzin, A.G. 2004. SCOP database in 2004: Refinements integrate structure and sequence family data. *Nucleic Acids Res.* **32**: D226–D229.
- Baker, D. and Sali, A. 2001. Protein structure prediction and structural genomics. *Science* **294**: 93–96.
- Benson, D.A., Karsch-Mizrachi, I., Lipman, D.J., Ostell, J., Rapp, B.A., and Wheeler, D.L. 2002. GenBank. *Nucleic Acids Res.* **30**: 17–20.
- Bentley, S.D., Chater, K.F., Cerdeno-Tarraga, A.M., Challis, G.L., Thomson, N.R., James, K.D., Harris, D.E., Quail, M.A., Kieser, H.,
- Harper, D., et al. 2002. Complete genome sequence of the model actinomycete *Streptomyces coelicolor* A3(2). *Nature* **417**: 141–147.
- Berman, H.M., Westbrook, J., Feng, Z., Gilliland, G., Bhat, T.N., Weissig, H., Shindyalov, I.N., and Bourne, P.E. 2000. The Protein Data Bank. *Nucleic Acids Res.* **28**: 235–242.
- Boeckmann, B., Bairoch, A., Apweiler, R., Blatter, M.C., Estreicher, A., Gasteiger, E., Martin, M.J., Michoud, K., O'Donovan, C., Phan, I., et al. 2003. The SWISS-PROT protein knowledgebase and its supplement TrEMBL in 2003. *Nucleic Acids Res.* **31**: 365–370.
- Burley, S.K. and Bonanno, J.B. 2003. Structural genomics. *Methods Biochem. Anal.* **44**: 591–612.
- Burley, S.K., Almo, S.C., Bonanno, J.B., Capel, M., Chance, M.R., Gaasterland, T., Lin, D., Sali, A., Studier, F.W., and Swaminathan, S. 1999. Structural genomics: Beyond the human genome project. *Nat. Genet.* **23**: 151–157.
- Chance, M.R., Sagi, I., Wirt, M.D., Frisbie, S.M., Scheuring, E., Chen, E., Bess Jr., J.W., Henderson, L.E., Arthur, L.O., South, T.L., et al. 1992. Extended x-ray absorption fine structure studies of a retrovirus: Equine infectious anemia virus cysteine arrays are coordinated to zinc. *Proc. Natl. Acad. Sci.* **89**: 10041–10045.
- Chance, M.R., Miller, L.M., Fischetti, R.F., Scheuring, E., Huang, W.X., Sclavi, B., Hai, Y., and Sullivan, M. 1996. Global mapping of structural solutions provided by the extended X-ray absorption fine structure ab initio code FEF 6.01: Structure of the cryogenic photoproduct of the myoglobin-carbon monoxide complex. *Biochemistry* **35**: 9014–9023.
- Chance, M.R., Bresnick, A.R., Burley, S.K., Jiang, J.S., Lima, C.D., Sali, A., Almo, S.C., Bonanno, J.B., Buglino, J.A., Boulton, S., et al. 2002. Structural genomics: A pipeline for providing structures for the biologist. *Protein Sci.* **11**: 723–738.
- Editorial. 2004. PSI-phase 1 and beyond. *Nat. Struct. Mol. Biol.* **11**: 201.
- Eswar, N., John, B., Mirkovic, N., Fiser, A., Ilyin, V., Pieper, U., Stuart, A.C., Marti-Renom, M.A., Madhusudhan, M.S., Yerkovich, B., et al. 2003. Tools for comparative protein structure modeling and analysis. *Nucleic Acids Res.* **31**: 3375–3380.
- Fiser, A., Sanchez, R., Melo, F., and Sali, A. 2001. Comparative protein structure modeling. In *Computational biochemistry and biophysics* (eds. M. Watanabe et al.), pp. 275–312. Marcel Dekker, NY.
- Gavin, A.C., Bosche, M., Krause, R., Grandi, P., Marzioch, M., Bauer, A., Schultz, J., Rick, J.M., Michon, A.M., Cruciat, C.M., et al. 2002. Functional organization of the yeast proteome by systematic analysis of protein complexes. *Nature* **415**: 141–147.
- Gerstein, M., Edwards, A., Arrowsmith, C.H., and Montelione, G.T. 2003. Structural genomics: Current progress. *Science* **299**: 1663.
- Goulding, C.W., Perry, L.J., Anderson, D., Sawaya, M.R., Cascio, D., Apostol, M.I., Chan, S., Parseghian, A., Wang, S.S., Wu, Y., et al. 2003. Structural genomics of *Mycobacterium tuberculosis*: A preliminary report of progress at UCLA. *Biophys. Chem.* **105**: 361–370.
- Guan, J., Almo, S.C., and Chance, M.R. 2004. Synchrotron radiolysis and mass spectrometry: A probe of the actin cytoskeleton. *Acta Chem. Res.* **37**: 221–229.
- Hasnain, S.S. 2004. Synchrotron techniques for metalloproteins and human disease in post genome era. *J. Synchrotron. Radiat.* **11**: 7–11.
- Hendrickson, W.A. 1991. Determination of macromolecular structures from anomalous diffraction of synchrotron radiation. *Science* **254**: 51–58.
- Holm, L. and Sander, C. 1995. Dali: A network tool for protein structure comparison. *Trends Biochem. Sci.* **20**: 478–480.
- . 1996. Mapping the protein universe. *Science* **273**: 595–603.
- John, B. and Sali, A. 2003. Comparative protein structure modeling by iterative alignment, model building, and model Assessment. *Nucleic Acids Res.* **31**: 3982–3992.
- Lesley, S.A., Kuhn, P., Godzik, A., Deacon, A.M., Mathews, I., Kreuzsch, A., Spraggon, G., Klock, H.E., McMullan, D., Shin, T., et al. 2002. Structural genomics of the *Thermotoga maritima* proteome implemented in a high-throughput structure determination pipeline. *Proc. Natl. Acad. Sci.* **99**: 11664–11669.
- Liu, J. and Rost, B. 2001. Comparing function and structure between entire proteomes. *Protein Sci.* **10**: 1970–1979.
- Lujan, H.D., Mowatt, M.R., Wu, J.J., Lu, Y., Lees, A., Chance, M.R., and Nash, T.E. 1995. Purification of a variant-specific surface protein of *Giardia lamblia* and characterization of its metal-binding properties. *J. Biol. Chem.* **270**: 13807–13813.
- Murzin, A.G., Brenner, S.E., Hubbard, T., and Chothia, C. 1995. SCOP: A structural classification of proteins database for the investigation of sequences and structures. *J. Mol. Biol.* **247**: 536–540.
- Orengo, C.A., Michie, A.D., Jones, S., Jones, D.T., Swindells, M.B., and Thornton, J.M. 1997. CATH—A hierarchical classification of protein domain structures. *Structure* **5**: 1093–1108.
- Pieper, U., Eswar, N., Stuart, A.C., Ilyin, V.A., and Sali, A. 2002. MODBASE, a database of annotated comparative protein structure

- models. *Nucleic Acids Res.* **30**: 255–259.
- Pieper, U., Eswar, N., Braberg, H., Madhusudhan, M.S., Davis, F., Stuart, A.C., Mirkovic, N., Rossi, A., Marti-Renom, M.A., Fiser, A., et al. 2004. MODBASE, a database of annotated comparative protein structure models, and associated resources. *Nucleic Acids Res.* **32**: D217–D222.
- Rajashankar, K., Chance, M.R., Burley, S.K., Jiang, J.S., Almo, S.C., Bresnick, A.R., Hunag, R., He, G., Chen, H., Sullivan, M., et al. 2001. Structural genomics at the National Synchrotron Light Source. *NSLS Activity Report* **2002**: 2–28 to 2–32.
- Reboul, J., Vaglio, P., Rual, J.F., Lamesch, P., Martinez, M., Armstrong, C.M., Li, S., Jacotot, L., Bertin, N., Janky, R., et al. 2003. *C. elegans* ORFeome version 1.1: Experimental verification of the genome annotation and resource for proteome-scale protein expression. *Nat. Genet.* **34**: 35–41.
- Sali, A. 1995. Comparative protein modeling by satisfaction of spatial restraints. *Mol. Med. Today* **1**: 270–277.
- . 1998. 100,000 protein structures for the biologist. *Nat. Struct. Biol.* **5**: 1029–1032.
- Sali, A., Glaeser, R., Earnest, T., and Baumeister, W. 2003. From words to literature in structural proteomics. *Nature Insight* **422**: 216–225.
- Sanchez, R. and Sali, A. 1998. Large-scale protein structure modeling of the *Saccharomyces cerevisiae* genome. *Proc. Natl. Acad. Sci.* **95**: 13597–13602.
- Sanchez, R., Pieper, U., Mirkovic, N., de Bakker, P.I., Wittenstein, E., and Sali, A. 2000. MODBASE, a database of annotated comparative protein structure models. *Nucleic Acids Res.* **28**: 250–253.
- Schaffer, A.A., Aravind, L., Madden, T.L., Shavirin, S., Spouge, J.L., Wolf, Y.I., Koonin, E.V., and Altschul, S.F. 2001. Improving the accuracy of PSI-BLAST protein database searches with composition-based statistics and other refinements. *Nucleic Acids Res.* **29**: 2994–3005.
- Shi, W., Ostrov, D., Gerchman, S., Kycia, H., Studier, W., Edstrom, W., Bresnick, A.R., Ehrlich, J., Blanchard, J., Almo, S.C., et al. 2003. High-throughput structural biology and proteomics. In *Protein chips, biochips, and proteomics: The next phase of genomics discovery*, Chapter 12, pp. 299–324. Marcel Dekker, NY.
- Stein, L.D., Bao, Z., Blasiar, D., Blumenthal, T., Brent, M.R., Chen, N., Chinwalla, A., Clarke, L., Clee, C., Coghlan, A., et al. 2003. The genome sequence of *Caenorhabditis briggsae*: A platform for comparative genomics. *PLoS Biol.* **1**: E45.
- Summers, M.F., Henderson, L.E., Chance, M.R., Bess Jr., J.W., South, T.L., Blake, P.R., Sagi, I., Perez-Alvarado, G., Sowder III, R.C., Hare, D.R., et al. 1992. Nucleocapsid zinc fingers detected in retroviruses: EXAFS studies of intact viruses and the solution-state structure of the nucleocapsid protein from HIV-1. *Protein Sci.* **1**: 563–574.
- Szpunar, J. 2004. Metalloomics: A new frontier in analytical chemistry. *Anal. Bioanal. Chem.* **378**: 54–56.
- Terwilliger, T.C., Park, M.S., Waldo, G.S., Berendzen, J., Hung, L.W., Kim, C.Y., Smith, C.V., Sacchettini, J.C., Bellinzoni, M., Bossi, R., et al. 2003. The TB structural genomics consortium: a resource for *Mycobacterium tuberculosis* biology. *Tuberculosis (Edinb)* **83**: 223–249.
- Tomba, P. 2002. Intrinsically unstructured proteins. *Trends Biochem. Sci.* **27**: 527–533.
- Tong, A.H., Lesage, G., Bader, G.D., Ding, H., Xu, H., Xin, X., Young, J., Berriz, G.F., Brost, R.L., Chang, M., et al. 2004. Global mapping of the yeast genetic interaction network. *Science* **303**: 808–813.
- Vitkup, D., Melamud, E., Moul, J., and Sander, C. 2001. Completeness in structural genomics. *Nat. Struct. Biol.* **8**: 559–566.
- Waterston, R.H., Lindblad-Toh, K., Birney, E., Rogers, J., Abril, J.F., Agarwal, P., Agarwala, R., Ainscough, R., Alexandersson, M., An, P., et al. 2002. Initial sequencing and comparative analysis of the mouse genome. *Nature* **420**: 520–562.
- Westbrook, J., Feng, Z., Jain, S., Bhat, T.N., Thanki, N., Ravichandran, V., Gilliland, G.L., Bluhm, W., Weissig, H., Greer, D.S., et al. 2002. The Protein Data Bank: Unifying the archive. *Nucleic Acids Res.* **30**: 245–248.
- Westbrook, J., Feng, Z., Chen, L., Yang, H., and Berman, H.M. 2003. The Protein Data Bank and structural genomics. *Nucleic Acids Res.* **31**: 489–491.
- Wheeler, D.L., Chappey, C., Lash, A.E., Leipe, D.D., Madden, T.L., Schuler, G.D., Tatusova, T.A., and Rapp, B.A. 2000. Database resources of the National Center for Biotechnology Information. *Nucleic Acids Res.* **28**: 10–14.
- Zhang, C. and Kim, S.H. 2003. Overview of structural genomics: From structure to function. *Curr. Opin. Chem. Biol.* **7**: 28–32.

## WEB SITE REFERENCES

- [www.nigms.nih.gov/psi/](http://www.nigms.nih.gov/psi/); NIH Web site providing information and relevant links for the Protein Structure Initiative.
- <http://targetdb.pdb.org/>; Web site operated by the Protein Databank to allow searching of targets from the structural genomics centers.
- [www.nysgxc.org/](http://www.nysgxc.org/); Web site operated by the NYSGRC. Its functions are to provide a public target list and progress as well as to allow consortium members to enter target data.
- <http://salilab.org/modbase/>; MODBASE, a comprehensive database of comparative protein structure models.
- [www-archbac.u-psud.fr/genomics/COG\\_Guess.html](http://www-archbac.u-psud.fr/genomics/COG_Guess.html); Clusters of Orthologous Groups Database Query Page to perform similarity search in COG database. This provides a function and COG category guess for input sequence.
- [http://salilab.org/modbase/models\\_nysgxc.html](http://salilab.org/modbase/models_nysgxc.html); Summary and statistics of homology modeling results using the NYSGXRC PDB structures as templates.

Received March 3, 2004; accepted in revised form May 12, 2004.